Spectrochimica Acta Part A: Molecular and Biomolecular Spectroscopy 200 (2018) 102–109

Contents lists available at ScienceDirect

Spectrochimica Acta Part A: Molecular and Biomolecular Spectroscopy

journal homepage: www.elsevier.com/locate/saa

Binding of p-mercaptobenzoic acid and adenine to gold-coated electroless etched silicon nanowires studied by surface-enhanced Raman scattering

Vlasta Mohaček-Grošev [a,*], Hrvoje Gebavi [a], Alois Bonifacio [b], Valter Sergo [b], Marko Daković [c], Danica Bajuk-Bogdanović [c]

[a] Centre of Excellence for Advanced Materials and Sensing Devices, Ruđer Bošković Institute, Bijenička cesta 54, 10002 Zagreb, Croatia
[b] University of Trieste, Via Valerio 6/A, Trieste, Italy
[c] Faculty of Physical Chemistry, University of Belgrade, Studentski trg 15-16, 11000 Belgrade, Serbia

ARTICLE INFO

Article history:
Received 21 July 2017
Received in revised form 30 March 2018
Accepted 9 April 2018
Available online 10 April 2018

Keywords:
Silicon nanowires
Normal mode analysis
Substrate binding
Biosensors
SERS
Mercaptobenzoic acid
Hot spots mapping

ABSTRACT

Modern diagnostic tools ever aim to reduce the amount of analyte and the time needed for obtaining the result. Surface-enhanced Raman spectroscopy is a method that could satisfy both of these requirements, provided that for each analyte an adequate substrate is found. Here we demonstrate the ability of gold-sputtered silicon nanowires (SiNW) to bind p-mercaptobenzoic acid in 10^{-3}, 10^{-4} and 10^{-5} M and adenine in 30 and 100 μM concentrations. Based on the normal mode analysis, presented here for the first time, the binding of p-mercaptobenzoic acid is deduced. The intensity enhancement of the 1106 cm^{-1} band is explained by involvement of the C—S stretching deformation, and the appearance of the broad 300 cm^{-1} band attributed to S—Au stretching mode. Adenine SERS spectra demonstrate the existence of the 7H tautomer since the strongest band observed is at 736 cm^{-1}. The adenine binding is likely to occur in several ways, because the number of observed bands in the 1200–1600 cm^{-1} interval exceeds the number of observed bands in the normal Raman spectrum of the free molecule.

1. Introduction

Since the discovery of surface-enhanced Raman scattering (SERS) by Fleischmann [1], Van Duyne [2], and Creighton [3], many research efforts have been dedicated to understand this effect [4–8]. Broadly speaking, SERS effect takes place if the metal substrate possesses an electronic state whose energy lies between the energy of the laser excitation and the energy of Raman scattered light, thus facilitating a "localized surface plasmon resonance" [9]. Originally the effect was studied first in colloidal silver [10] and gold nanoparticles aggregates [11], reaching a sensitivity down to single molecule detection [12,13].

The possibilities of SERS effect on solid substrates have soon surpassed those of free flowing aggregates, because of better reproducibility [14–16]. The importance of nanoscale dimensions of metal particles has been investigated and repeatedly proven essential for the SERS to take place [17,18]. Besides electromagnetic contribution to enhancement, a chemical one is often mentioned, but it is several orders of magnitude smaller [4]. Few molecules with strong resonant Raman spectrum have become very popular for testing substrates – one is rhodamine 6G, another crystal violet. Both of them incorporate several aromatic rings having delocalized electron orbitals. The UV VIS spectrum of crystal violet, for example, changes dramatically depending on the pH of the solution. When the pH is 1, the absorbance has its maximum in the blue spectral region, while it shifts to red if the pH changes to 4 [19]. Still, when testing new substrates it is advisable to check their properties with non-resonant molecules [9].

Among numerous applications of SERS, the possibility of detecting an extremely small quantity of an analyte in blood, urine or saliva within minutes has attracted a lot of attention, and has been a part of study effort within the COST action [20]. Two main strategies offer themselves: the first is to devise a label-free method of detection, thus concentrating on a substrate itself [21], and the second one is to devise a chemical marker which binds to the analyte and to the substrate and through which one ascertains the existence of analyte [22,23].

Here we present the results of a joint effort to produce a reliable substrate with good reproducibility based on electroless chemical etching method. This method dates from 2002 [24]., is cost effective and produces silicon nanowires 50–100 nm in diameter and several tens of μm in length [25–37]. In contrast to electrochemical etching that is

* Corresponding author.
E-mail address: Vlasta.Mohacek.Grosev@irb.hr. (V. Mohaček-Grošev).

https://doi.org/10.1016/j.saa.2018.04.016
1386-1425/

also often used, here there is no external voltage applied in electrochemical cell, but hydrogen fluoride or ammonia fluoride providing excess electrons to ionize silver atoms [25–27]. Gold particles are added on the top of the substrate, thus creating optimal binding surface for Raman spectroscopy with near infrared (785 nm) laser. Welding of a silicon nanowire with a gold droplet produces an atomic force microscopy tip that serves as a probe for tip-enhanced Raman spectroscopy (TERS) [28–30]. We present SERS spectra of p-mercaptobenzoic acid (4MBA), and discuss possible types of molecular binding. By performing normal coordinate calculation, we elucidate the nature of observed spectral changes which appear on binding of 4MBA to the substrate.

2. Experimental

Silicon wafers - (100) orientation – single crystalline p-type, were cleaned with standard RCA (Radio Corporation of America) cleanup processes. The mixture of hydrofluoric acid (5 M) and $AgNO_3$ solution under UV lamp was utilized for synthesizing silicon nanowires by electroless wet chemical etching method during period of 90 min. The experiment was carried at ambient temperature of 26^0C. After etching, the samples were covered with grey silver layer which was removed with NH_4OH:H_2O_2:H_2O solution using the 1:1:5 volume-to-volume ratio. The samples were rinsed with MQ water and dried. Next step included gold sputtering of silicon nanowires during various time intervals. For the etching of the first group of samples the 30 mM concentration of $AgNO_3$ was used, the sputtering was performed during 1, 10, 15 or 20 min and all were annealed at 650^0C in the oven under argon flow for one hour. The second group of substrates was etched using two concentrations of $AgNO_3$: 10 and 30 mM, they were sputtered during 7, 10, 15 or 20 min. Samples from the second group were further divided into one half that was annealed at 650^0C, while the other half which was not annealed.

2.1. Gold coating

For sputtering a Polaron E5000 sputter coater was used. The vacuum obtained prior to Au sputtering was 10^{-5} mbar. During the sputtering argon plasma was utilized and the pressure inside the

Table 1
Calculated normal modes of 4MBA with potential energy distribution are compared with Raman and infrared bands observed for crystalline powder and SERS spectrum obtained for not annealed substrate from Fig. 5 (cm^{-1}). The multiplicity of observed bands is greater than one (such as for C═O stretching) because of crystal splitting. Notation of internal coordinates is explained in Supplementary Material.

Mode		Observed (crystal)		Observed (SERS)
		Raman	Infrared	
A'				
3763	100 l	Not acq.	Not acq.	Not acq.
3228	100 r	Not acq.	Not acq.	Not acq.
3219	100 r	Not acq.	Not acq.	Not acq.
3194	100 r	Not acq.	Not acq.	Not acq.
3191	100 r	Not acq.	Not acq.	Not acq.
2694	100 s	Not acq.	Not acq.	Not acq.
1783	81 D	1676,1655, 1643,1638	1694, 1679,1652	1689
1644	67 R + 21 Φ + 10 Ω	1632,1624,1615	1593	
1604	74 R + 10 Φ	1599	1564	1589
1529	59 Φ + 34 R	1456	1493	
1445	51 R + 40 Φ	1405	1444, 1424, 1402	1482
1376	26 ε + 21 d + 18 CC + 18κ			1414
1346	76 R+ 13 Φ	1322	1323, 1308	
1333	73 Φ + 23 R	1296	1296	
1223	47 Φ + 22 R + 21 ε	1286	1281,1263, 1232	1281
1194	36 Φ + 31 ε + 13 R	1185	1182	1178
1144	60 Φ + 33 R	1138	1130	
1120	28 R + 26d +16 Φ		1115	
1106	56 R + 19 d + 13 S	1100	1096, 1086, 1051	1077
1030	61 Ω + 27 R	1075	1015	1014
944	91 δ_S	914	956, 925	
793	29 R + 29 Ω + 15 CC	804	831, 805	802
672	36 κ + 21 Ω + 14 S	700	710	692
644	83 Ω + 10 R	635	632	631
520	29 η + 23 S + 13 CC		546	
496	27 κ + 23 η + 14 δ_C		518	
308	37 Ω + 17 S + 16 CC + 12 κ	344		335
298	54 δ_S + 15 κ + 13 δ_C	276		298
168	52 CC+ 22 S + 18 κ	186		
Mode	PED (%)	Observed (crystal)		Observed (SERS)
		Raman	Infrared	
A″				
991	100 μ			
978	100 μ		974	
851	71 μ + 30 μSC	818	848	848
841	98 μ	812	848	
765	70 μSC + 29 μ		757	763
680	93 δ		684	716
595	85 τOH + 11 δ		576	
472	47 δ + 46 μSC		470	407
414				
259	80 μSC + 19 δ	249		
156	100 τSC	223,205		
88	56 δ + 44 μCC	84		
71	97 τOCCC	79		

chamber was $4 \cdot 10^{-4}$ mbar. The Au layer thickness is estimated to increase linearly with time, and is assumed to be between 100 and 150 nm for 40 min of sputtering.

2.2. Raman measurements

Raman experiments were conducted on four instruments: T64000 Horiba Jobin-Yvon with 670 nm laser for **powder sample** of 4MBA, Thermo Scientific DXR Raman microscope with 785 laser illumination which was used for SERS **droplet experiments**, BWTek i-Raman Plus with 785 nm laser for SERS **immersion experiments**, and Renishaw InVia spectrometer with 785 nm laser source for Raman mapping. Each of these four setups is described in detail:

2.3. Raman and infrared spectra of polycrystalline 4MBA

Polycrystalline powder of 4-MBA was put on a glass slide under microscope of HORIBA Jobin Yvon T64ooo Raman spectrometer operating in triple subtractive mode, using 670 nm red excitation laser line with power of 3 mW on the sample. Spectral resolution was 0.6 cm^{-1} and the spot size 1 μm. Infrared spectra of 4MBA powder pressed in KBr pellet were obtained in transmission by Perkin Elmer Spectrum GX mode, with 20 repetitions and 4 cm^{-1} resolution. The observed bands are reported in Table 1.

2.4. Raman SERS spectra of the first group of substrates – droplet method

The SERS spectra using the annealed substrates etched for 1, 10, 15 or 20 min with 5 M HF/30 mM $AgNO_3$ were obtained by leaving a 1 μl droplet of 0.01 M 4MBA on a surface and recording the Raman signal immediately using Thermo Scientific DXR Raman microscope operating with 785 nm laser excitation line. Spectral resolution of this instrument was 4 cm^{-1}. The acquisition time was 10 s, the pinhole was 50 μm, and four accumulations were performed. In order to test the limit of detection SERS spectra of droplets from 10^{-3} M, 10^{-4} M and 10^{-5} M solutions of 4MBA were recorded.

2.5. Raman SERS spectra of the second group of substrates – immersion method

Substrates from the second group were immersed either into a 1 mM 4MBA water solution, or into 30 μM or 100 μM adenine water solution for 30 min, taken out, rinsed and dried. SERS spectra using the substrates of the second group were recorded by portable BWTek i-Raman Plus spectrometer using 20× objective and 785 nm excitation suitable for gold sputtered surfaces, with spectral resolution of 4 cm^{-1}. The spot diameter was 80 μm, the acquisition time 5 s and a single accumulation of the spectrum undertaken. Besides 1 mM 4MBA concentration, a sensitivity test included 10^{-4} M, 10^{-5} M, 10^{-6} M and 10^{-7} M 4MBA water and ethanol solutions.

2.6. Raman mapping

The spectral mapping of the 1520–1640 cm^{-1} Raman interval of 4MBA was performed with Renishaw INVIA spectrometer, operating with 785 nm laser source, on two selected substrates, both etched with 5 M HF and 30 mM $AgNO_3$ solution, sputtered for 20 min with gold, one annealed and the other not annealed. The intensity maps were analyzed using the HyperSpec package [39] for R [40].

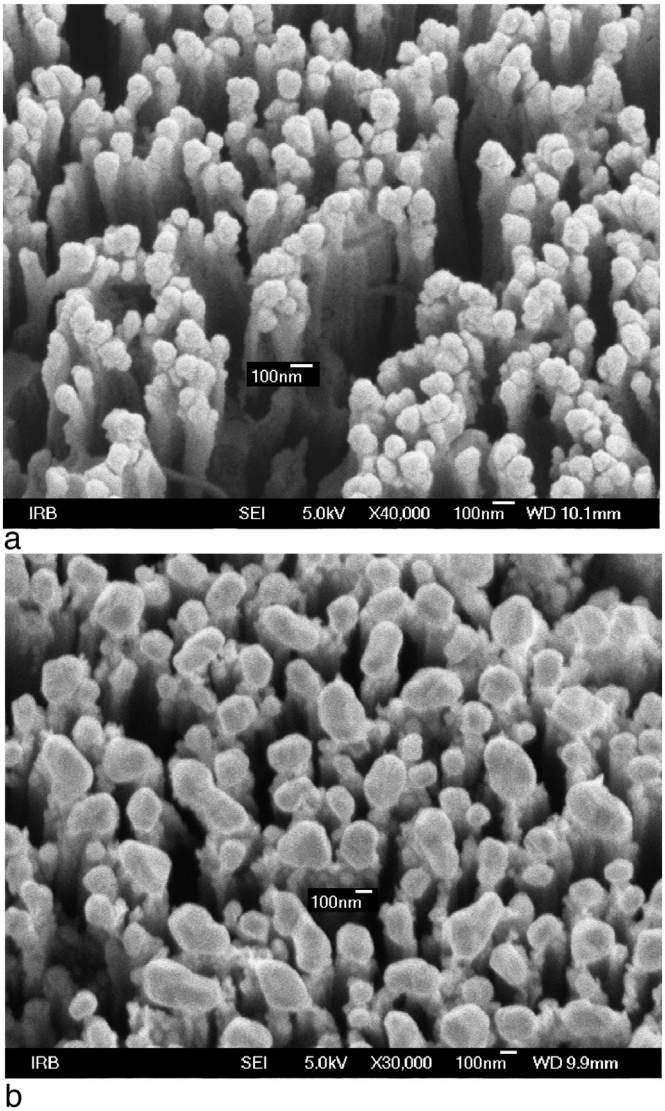

Fig. 1. Scanning electron microscopic images of silicon nanowires obtained by electroless chemical etching (30 mM $AgNO_3$/5 M HF solution) with gold sputtered for 20 min. a) not annealed substrate, b) substrate annealed at 650 °C for 1 h in argon atmosphere. The bar corresponds to 100 nm. The tilt angle was 15°. (For interpretation of the references to colour in this figure legend, the reader is referred to the web version of this article.)

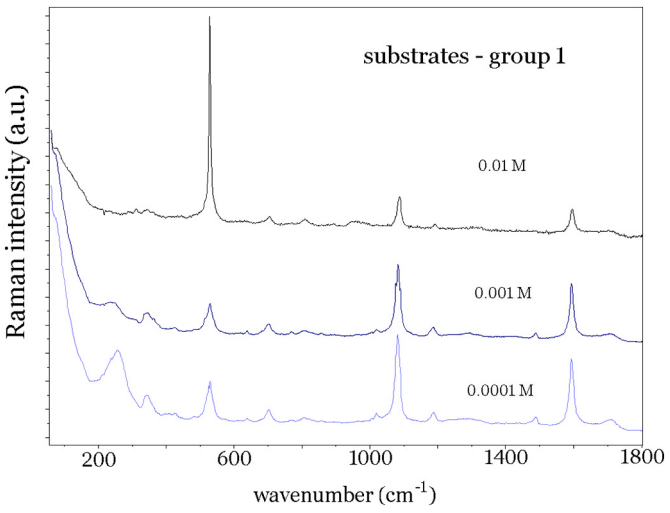

Fig. 2. Comparison of SERS spectra of wet droplets of 4MBA ethanol solution on AuNP@SiNW substrates. Laser excitation: 785 nm, Thermo Scientific DXR Raman spectrometer.

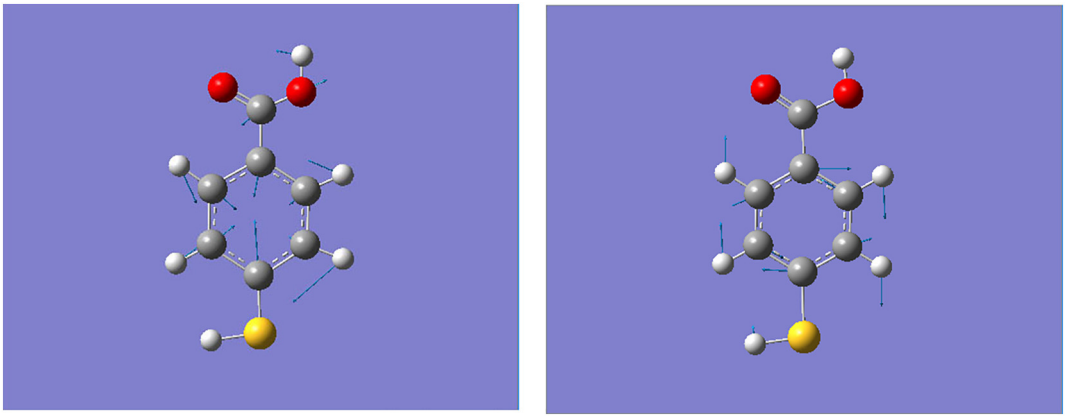

Fig. 3. Arrows indicate movements of atoms in the two strongest normal modes of free 4MBA: calculated at 1106 (left) and 1604 cm^{-1} (right).

2.7. Scanning electron microscopy

Scanning electron microscopy of silicon nanowires substrates was performed using JEOL field emission SEM, model JEOL JSM-7000F, with acceleration voltage of 5 kV.

2.8. Computational details

Optimization of the geometry of the 4-mercaptobenzoic acid was performed using Gaussian03 program [41], utilizing the implemented density functional theory through Becke exchange and Lee, Yang and Parr correlation functionals with 6-311G(d,p) basis set. The subsequent normal modes calculation proved that the geometry was indeed a stable state and no imaginary frequencies occurred. Introducing internal coordinates suitable for a planar molecule such as 4MBA, we used MOLVIB program by Krisztof Kuczera [42] and obtained a potential energy distribution among normal modes. Details of this calculation are part of the Supplementary Material.

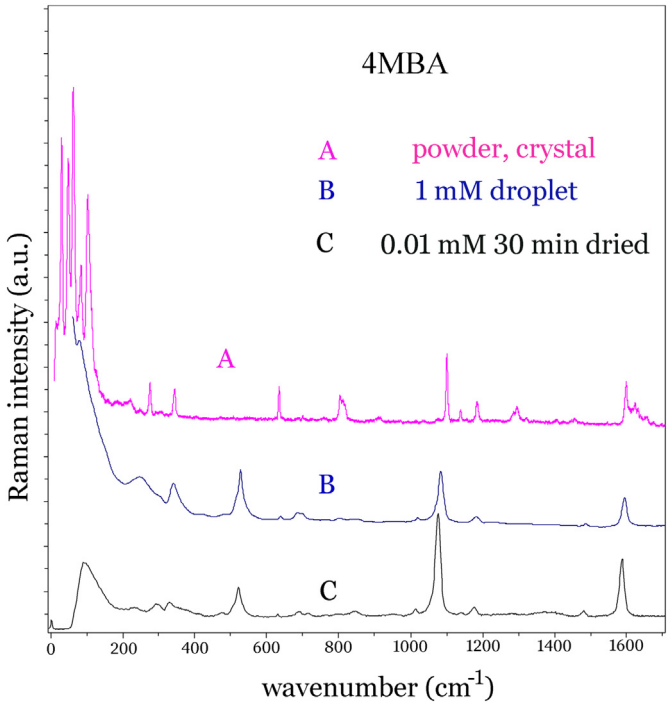

Fig. 4. Comparison of Raman spectrum of polycrystalline 4MBA (A) obtained with 670 nm laser, with the SERS spectrum of 1 mM 4MBA droplet (B), and the SERS spectrum obtained by immersion of the substrate in the 0.01 mM ethanol solution of 4MBA for 30 min, rinsed and dried (C). (B) and (C) were obtained with 785 nm excitation.

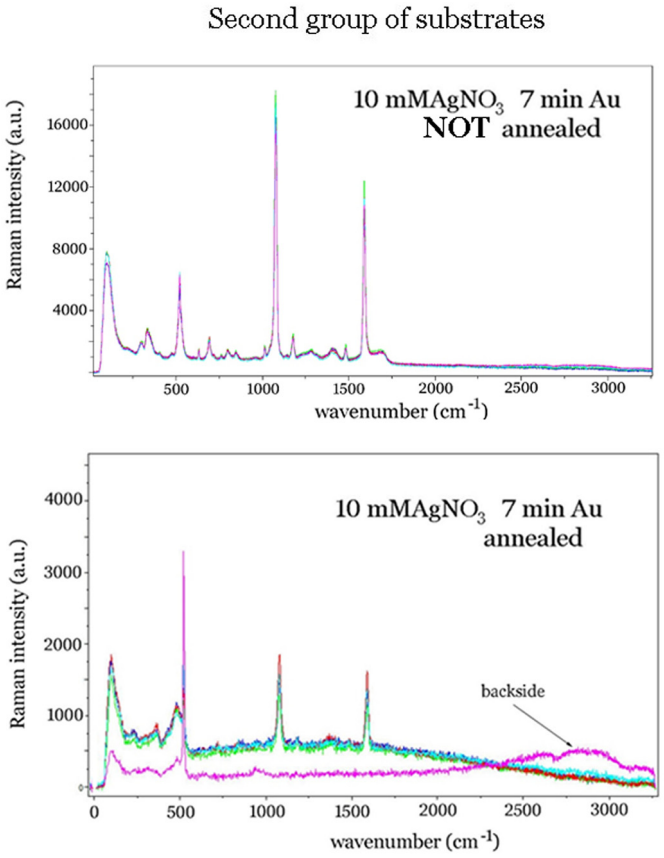

Fig. 5. SERS spectra of 1 mM solution of 4MBA (substrates were submerged for 30 min in 0.001 M 4MBA solution in EtOH, rinsed and dried) with 785 nm excitation using 20× objective, 5 s accumulation time and 1 repetition, with BWTek i-plus spectrometer. Spectra shown above were taken on different points on a single substrate which was not annealed, spectra shown below on an annealed substrate. Spectrum of the backside of the same substrate is also shown.

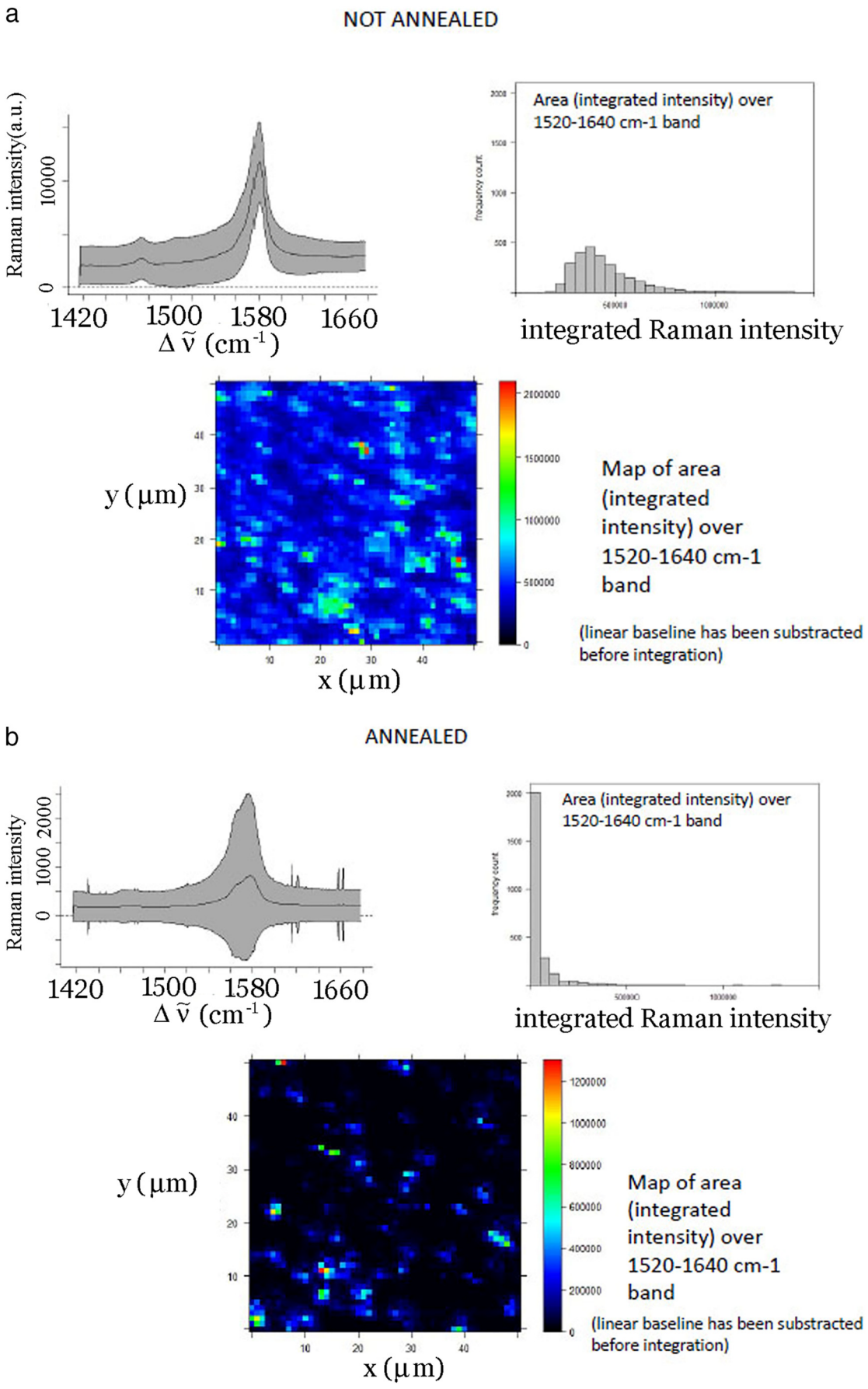

Fig. 6. a) Results of the mapping of not annealed AuNP/SiNW substrate immersed in 1 mM solution of 4MBA (30 mM $AgNO_3$, 20 min sputtering Au). b) Results of the mapping of annealed AuNP/SiNW substrate immersed in 1 mM solution of 4MBA and rinsed (30 mM $AgNO_3$, 20 min sputtering Au).

3. Results and Discussion

Scanning electron microscopic images of two selected substrates from the second group are displayed in Fig. 1. The diameters of silicon nanowires (SiNW) were 80 to 100 nm, and their length from 1 to 1.1 μm. The wires ran parallel to each other, occasionally producing entanglements, while their free ends were accessible to gold particles sputtered onto them. The voids between SiNWs grow larger when etching time exceeds 1 h. The appearance of voids described by Bontempi et al. [31] was attributed to mechanical damage because SiNWs became brittle. The procedures of electroless chemical etching and metal-assisted chemical etching refer to mainly the same procedure, sometimes without hydrogen peroxide H_2O_2 and sometimes exchanging HF with NH_4F [24–38]. Occasionally nanowires get entangled or joined at the top. The effect this has on SERS spectrum was discussed by Kara et al. [36] in their SERS spectrum of melamine. The strongest Raman band obtained with substrate with non-leaning SiNWs corresponded to the strongest band in the reference Raman spectrum of pure melamine (676 cm^{-1}), while there were two strong bands obtained with substrate with leaning SiNWs, one shifted to 712 cm^{-1} and one not-much-shifted from the reference (680 cm^{-1}).

When chloroauric acid, $HAuCl_4 \cdot 3H_2O$, is used for chemical deposition of gold on silicon nanowires, gold particles enter the vertical space between the wires, getting bigger towards the top [32–34]. Our hybrid sensors were produced by sputtering gold onto SiNWs, thus gold nanoparticles (AuNP) formed predominantly at SiNW tips. Their dimensions were in the range 120 to 230 nm, while annealing caused coalescence of several AuNPs into a bigger one (Fig. 1.)

The suitability of our hybrid substrates for SERS is demonstrated in Fig.2, where droplets of different concentrations of 4MBA were deposited on a AuNP@SiNWs, which were not annealed. Spectra of droplets were recorded while the samples were still wet, focusing the image on the substrate/droplet interface. As the concentration of 4MBA is lowered, the band at 300 cm^{-1} that corresponds to the calculated value of 298 cm^{-1} for C—C—S in plane deformation is gaining the intensity.

The band at 528 cm^{-1} corresponds to the A_g mode of the silicon, but is shifted from the value observed for crystal (520.7 cm^{-1}). Also, shoulders appear on this band, probably coming from the 518 and 548 cm^{-1} modes observed in the infrared spectrum and too weak to be observed in normal Raman spectrum (Table 1, Supplementary Fig. S1). The two strongest 4MBA bands are observed at 1077 and 1589 cm^{-1}, and the normal modes assigned to them depicted in Fig. 3.

The droplet technique is compared with immersion and drying technique in Fig. 4. The substrate is immersed in solution for 30 min, then taken out, rinsed and left to dry. The crystal structure of 4MBA is unknown, therefore we could not calculate the positions of phonon bands for powder sample (spectrum A, Fig. 4.). The observed bands at

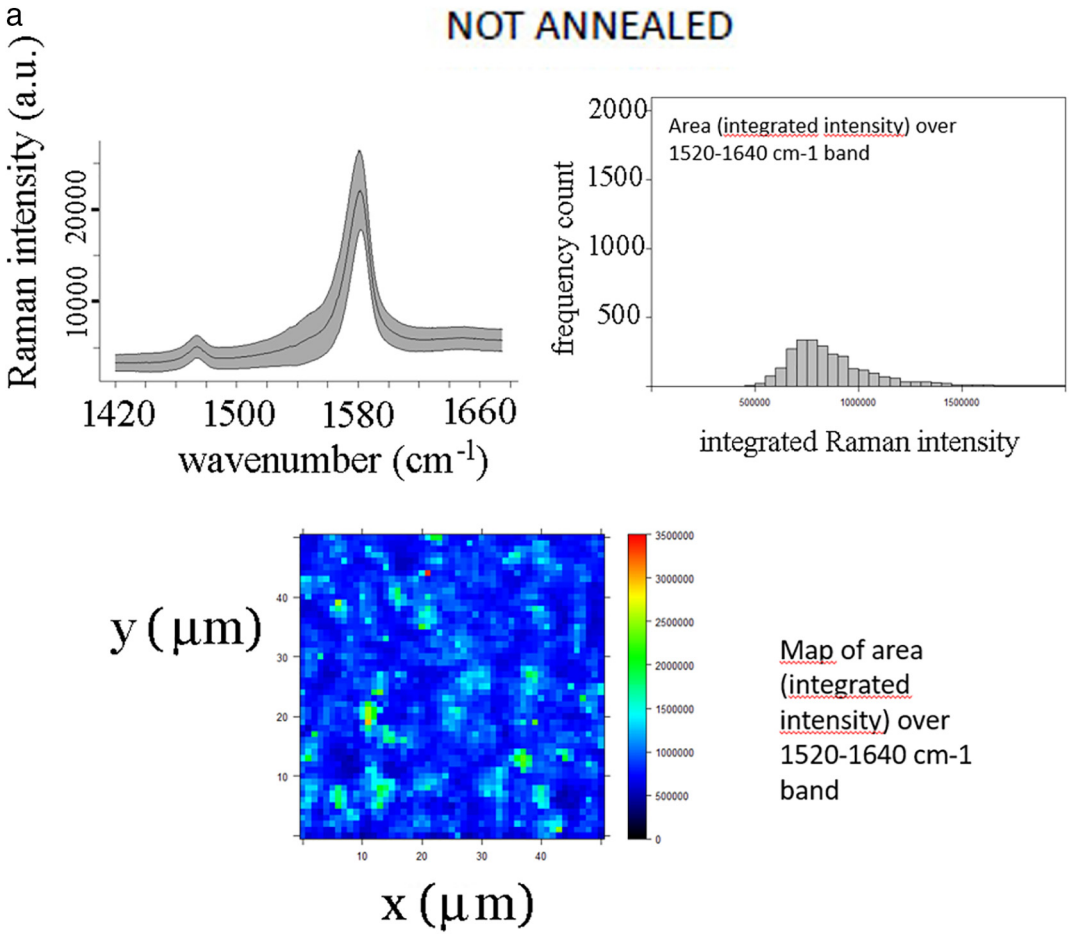

Fig. 7. Comparison of SERS spectroscopy on gold-coated and pure vertical silicon nanowires. We used 40 mM $AgNO_3$/5 M HF solution, and cut the plate in two pieces. On the first part the gold was sputtered for 7 min. The height of these vertical Si nanowires was 800 nm. Concentration of 4MBA: 10^{-4} M. a) Gold-coated not annealed SiNW. Above left: average Raman spectral intensity is the middle line, the upper and lower spectrum bordering the grey area mark standard deviation of intensity. Above right: distribution of number of integrated Raman intensity between 1520 and 1640 cm^{-1} of the mapped area. Below left: colour map with hot spots in light blue and yellow. The Raman intensity corresponding each colour is given in the legend on the right. b) Pure SiNW. Above left: average Raman spectral intensity is the middle line, the upper and lower spectrum bordering the grey area mark standard deviation of intensity. Above right: distribution of number of integrated Raman intensity between 1520 and 1640 cm^{-1} of the mapped area. Below left: colour map with hot spots in light blue and yellow. The Raman intensity corresponding each colour is given in the legend on the right. (For interpretation of the references to colour in this figure legend, the reader is referred to the web version of this article.)

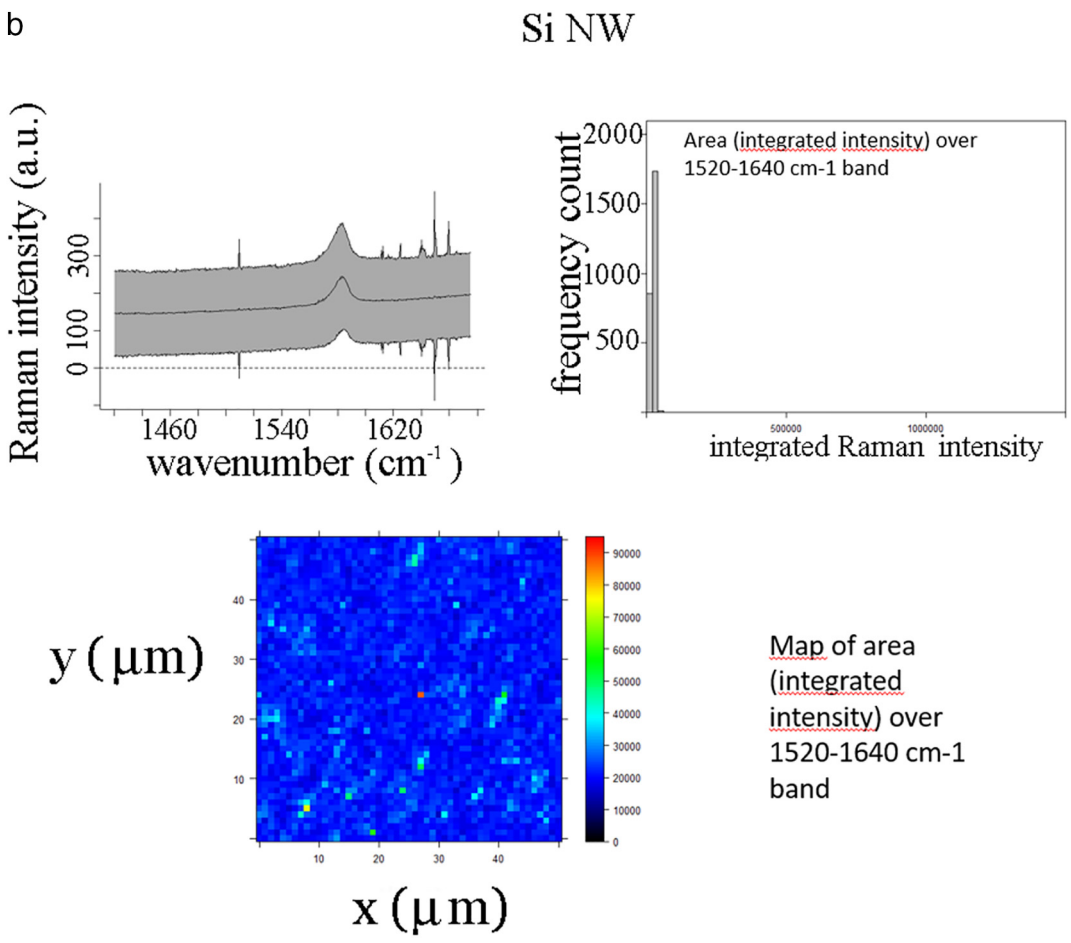

Fig. 7 (*continued*).

276 and 344 cm^{-1} are most probably internal molecular modes, since there exist three modes predicted for free 4MBA at 259, 298 and 308 cm^{-1} (see Table 1 where all calculated modes for free 4MBA are compared with the observed bands positions). The mode calculated at 259 cm^{-1} is out-of-plane deformation, while 298 cm^{-1} mode is C—C—S bending deformation coupled with C—C—O bending deformation of the carboxylic group. The 308 cm^{-1} mode is also an in-plane mode containing ν(C—S) and ν(C—COOH) stretching motions. In SERS spectra from Fig. 5, bands at 298 and 335 cm^{-1} observed for not annealed substrates gain in the intensity. The shift of 27 cm^{-1} between the expected value of 308 cm^{-1} for free molecule and the observed band at 335 cm^{-1}in SERS spectrum points to the fact that binding to the gold-coated silicon nanowire substrate has taken place. Comparing not annealed and annealed substrates, we find that there are no bands at 298 cm^{-1} and 335 cm^{-1}, but an asymmetric weaker band at 360 cm^{-1} in the case of annealed substrate (Fig. 5). This change is attributed to much bigger gold islands on the top of Si nanowires (Fig. 1).

Para-mercaptobenzoic acid is a suitable SERS test molecule able to bind both on gold and silver nanoparticles [43–47]. It was one of several benzoic acid derivatives for which Guo et al. performed time-dependent density functional theory calculation of possible HOMO and LUMO states [48]. It turns out that at different pH, LUMO available orbital has different electron density, for low pH it is spread over all molecule, while for high pH it is almost exclusively localized on —S—H group. Michota and Bukowska used roughened silver or gold electrodes at various voltages for obtaining SERS spectra of 4MBA [44]. When gold surfaces were prepared, 4MBA attached itself with sulphur atom to the gold one, irrespectively of pH. They observed two bands characteristic for —COO^- group, the symmetric stretching band at 1370–1380 $cm^{-1,}$ and the bending of COO^- group at 848 cm^{-1}. These two bands occur when pH is approximately neutral, and we have recorded them in our SERS spectra of 10^{-5} M 4MBA (spectrum C, Fig. 4., and Supplementary Fig. S2). The absence of 2580 cm^{-1} band assigned to ν(S—H) is conclusive of binding via sulphur atom (Fig. 5).

Raman mapping of an annealed vs. not-annealed substrate was performed in order to explain the better quality of SERS spectra in not-annealed samples (Fig.5). In Fig. 6a and Fig. 6b the density of hot spots is compared by analyzing the integrated Raman intensity of the 1520–1640 cm^{-1} 4MBA band.

Not-annealed substrates presented a more homogeneous distribution of hot spots with respect to annealed ones, according to intensity maps and area distribution histograms in Fig.6. In annealed substrates, high intensity values are only observed but in few isolated spots, on a background of low-intensity values. On the other hand, in non-annealed substrates, the dimensions of the high-intensity spots were larger, on an overall background of medium-intensity values. It seems that larger dimensions of the nanostructures obtained by annealing with respect to non-annealed substrates (as seen in Fig.1) are less efficient in enhancing the signal. Their structural inhomogeneity exists on a larger scale, leading to a worse intra-substrate repeatability.

In order to experimentally determine the ratio of Raman intensity for gold-coated not annealed silicon nanowires and pure silicon nanowires, we performed Raman mapping of the two substrates previously immersed into 10^{-4} M solution of 4MBA for 30 min and dried. The intensity ratio of the background corrected average SERS spectra is 234

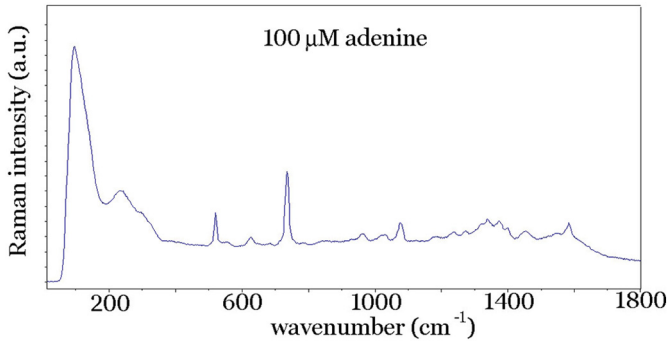

Fig. 8. SERS spectrum of 100 μM solution of adenine on AuNP@SiNW substrate cleaned with 30 mM $AgNO_3$, sputtered with gold for 7 min, not annealed. Recorded with BwTek spectrometer, 785 nm excitation. Low frequency band at 100 cm^{-1} is an artefact due to notch filter. (For interpretation of the references to colour in this figure legend, the reader is referred to the web version of this article.)

(Fig. 7a and b). This is thus our estimate of the enhancement factor, assuming the same number of molecules is covering the area of mapped surfaces.

In Fig.8, a SERS spectrum of 100 μM concentrated solution of adenine obtained on not annealed substrate is shown. We used it to test the usability of these substrates with another non-resonant analyte, and in particular for an analyte lacking a thiol —SH group. Adenine is a DNA base, a planar molecule with several —NH groups able to participate in hydrogen bonding. Since adenine disposes with two tautomers in neutral form, it is of interest to note that the strongest band we observed lies at 736 cm^{-1}, corresponding to N7 tautomer in the notation of Pagliai et al. [49].

4. Conclusion

The gold-sputtered not annealed silicon nanowire hybrid substrates for surface-enhanced Raman scattering presented in this work have been proved highly efficient sensors for organic molecules disposing with thiol group. Para-mercaptobenzoic acid (4MBA) SERS spectra were compared with Raman and infrared spectra of polycrystalline powder and assigned with the help of normal coordinate calculation which followed an ab initio optimization of electronic and nuclear configuration. At neutral pH, 4MBA binds to gold on not annealed substrates, the bands at 298 and 335 cm^{-1} gaining the intensity. These two bands are assigned to in-plane C—C—S bending and C—S stretching band. The stretching of S—H (expected at cca 2550 cm^{-1}) is never observed in any SERS spectrum.

The bending of C—O—H is predicted to contribute to two normal modes, 1223 and 1194 cm^{-1}. The corresponding observed broad SERS band is centered around 1281 cm^{-1}.

Surface distribution of substrate hot spots was obtained via Raman mapping of the 1520–1640 cm^{-1} interval both for annealed and not annealed substrates. Not annealed substrates proved to have more homogeneous distribution of hot spots and served as better enhancers of Raman signal.

Supplementary data to this article can be found online at https://doi.org/10.1016/j.saa.2018.04.016.

Acknowledgement

This work was supported by COST action BM1401, Raman-based applications for clinical diagnostics (Raman4Clinics)" through two short-term missions. This work has been partly supported by Croatian Science Foundation under the Project No. IP-2014-09-7046 and by SAFU project KK.01.1.1.01.0001. Computations were performed at the University of Zagreb Computing Centre SRCE.

References

[1] M. Fleischmann, P.J. Hendra, A.J. McQuillan, Chem. Phys. Lett. 26 (1974) 163.
[2] D.L. Jeanmaire, R.P. van Duyne, J. Electroanal. Chem. 84 (1977) 1.
[3] M.G. Albrecht, J.A. Creighton, J. Am. Chem. Soc. 99 (1977) 5215.
[4] M. Moskovits, Rev. Mod. Phys. 57 (1985) 783.
[5] M. Moskovits, Phys. Chem. Chem. Phys. 15 (2013) 5301–5311.
[6] F.S. Ameer, C.U. Pittman, D. Zhang, J. Phys. Chem C 117 (2013) 27096.
[7] Y.S. Yamamoto, T. Itoh, J. Raman Spectrosc. 47 (2016) 78–88.
[8] Surface-Enhanced Raman Scattering, H. Kneipp, M. Moskovits, in: K. Kneipp (Ed.), Topics in Applied Physics, 103, Springer Verlag, 2006.
[9] B. Sharma, M. Fernanda Cardinal, S.L. Kleinman, N.G. Greeneltech, R.R. Frontiera, M.G. Blaber, G.C. Schatz, R.P. Van Duyne, MRS Bull. 38 (2013) 615–624.
[10] P. Hildebrandt, M. Stockburger, J. Phys. Chem. 88 (1984) 5935–5944.
[11] A.M. Schwartzberg, C.D. Grant, A. Wolcott, C.E. Talley, T.R. Huser, R. Bogomolni, J.Z. Zhang, J. Phys. Chem. B 108 (2004) 19191–19197.
[12] K. Kneipp, H. Kneipp, J. Kneipp, Acc. Chem. Res. 39 (2006) 443–450.
[13] S.L. Kleinmann, E. Ringe, N. Valley, K.L. Wustholz, E. Phillips, K.A. Scheidt, G.C. Schatz, R.P. Van Duyne, J. Am. Chem. Soc. 133 (2011) 4115–4122.
[14] A. Dhawan, M. Gerhold, Y. Du, V. Misra, T. Vo-Dinh, Proc of SPIE 7205 (2009) 72050S–1.
[15] A.X. Wang, X. Kong, Dent. Mater. 8 (2015) 3024–3052.
[16] M. Jahn, S. Patze, I.J. Hidi, R. Knipper, A.I. Radu, A. Mühlig, S. Yüksel, V. Peksa, K. Weber, T. Mayerhöfer, D. Cialla-May, J. Popp, Analyst 141 (2016) 756–793.
[17] D.-K. Lim, K.-S. Jeon, H.M. Kim, J.-M. Nam, Y.D. Suh, Nat. Mater. 9 (2010) 60–67.
[18] J.M. McMahon, S. Li, L.K. Ausman, G.C. Schatz, J. Phys. Chem. C 116 (2012) 1627–1637.
[19] L. Angeloni, G. Smulevich, M.P. Marzocchi, J. Raman Spectrosc. 8 (1979) 305.
[20] COST, Action BM1401: Raman-based applications for clinical diagnostics (Raman4clinics), https://www.raman4clinics.eu/.
[21] A. Bonifacio, S. Cervo, V. Sergo, Anal. Bioanal. Chem. 407 (2015) 8265.
[22] L. Wu, Z. Wang, K. Fan, S. Zong, Y. Cui, Small 11 (2015) 2798–2886.
[23] S. Chen, Y. Yuan, S. Han, R. Gu, Chem. Commun. 47 (2011) 4225.
[24] K.-Q. Peng, Y.-J. Yan, S.-P. Gao, J. Zhu, Adv. Mater. 14 (2002) 1164.
[25] C. Benoit, S. Bastide, C. Lévy-Clément, ECS Trans. 16 (2008) 245.
[26] N. Megouda, T. Hadjersi, S. Szunerits, R. Boukherroub, Appl. Surf. Sci. 284 (2013) 894.
[27] V. Sivakov, F. Voigt, B. Hoffmann, V. Gerliz, S. Christiansen, Intech "Nanowires Fundamental Research"ISBN 978-953-307-327-9, Chapter 3 2011.
[28] M. Becker, V. Sivakov, G. Andrä, R. Geiger, J. Schreiber, S. Hoffmann, J. Michler, A.P. Milenin, P. Werner, S.H. Christiansen, Nano Lett. 7 (2007) 75–80.
[29] M. Becker, V. Sivakov, U. Gösele, T. Stelzner, G. Andrä, H.J. Reich, S. Hoffmann, J. Michler, S.H. Christiansen, Small 4 (2008) 398–404.
[30] P.R. Brejna, P.R. Griffiths, Appl. Spectrosc. 64 (2010) 493–499.
[31] N. Bontempi, M. Salmistraro, M. Ferroni, L.E. Depero, I. Alessandri, Nanotechnology 25 (2014), 465705.
[32] X. Yang, H. Zhong, Y. Zhu, J. Shen, C. Li, Dalton Trans. 42 (2013) 14324–14330.
[33] W. Ming-Li, Z. Chang-Xing, W. Zheng-Long, J. Xi-Li, X. Hai-Jun, Chin. Phys. B. 23 (2014), 067802.
[34] H. Wang, X. Jiang, S.-T. Lee, Y. He, Small 10 (2014) 4455–4468.
[35] A. Convertino, V. Mussi, L. Maiolo, Nature Scientific Reports 6 (2016) 25099.
[36] S.A. Kara, A. Keffous, A.M. Giovanozzi, A.M. Rossi, E. Cara, L. D'Ortenzi, K. Sparnacci, L. Boarino, N. Gabouze, S. Soukane, RSC Adv. 6 (2016) 93649.
[37] H. Cui, S. Li, S. Deng, H. Chen, C. Wang, ACS Sensors 2 (2017) 386–393.
[38] H. Gebavi, L. Mikac, M. Marciuš, M. Šikić, V. Mohaček-Grošev, T. Janči, S. Vidaček, E. Hasanspahić, E. Omanović Miklićanin, M. Ivanda, Silicon nanowires substrates fabrication for ultra-sensitive surface enhanced Raman spectroscopy sensors, Croat. Chem. Acta 90 (2017) 256–262.
[39] C. Beleites, V. Sergo, Hyperspec: A package to handle hyperspectral data in R, R Package version 0.98-201-50304, 2015 http://hyperspec.r-forge.r-project.org.
[40] R Core Team, R: A Language and Environment for Statistical Computing, R Foundation for Statistical Computing, Vienna, Austria, 2016 https://www.R-project.org/.
[41] M.J. Frisch, G.W. Trucks, H.B. Schlegel, G.E. Scuseria, M.A. Robb, J.R. Cheeseman, J.A. Montgomery Jr., T. Vreven, K.N. Kudin, J.C. Burant, J.M. Millam, S.S. Iyengar, J. Tomasi, V. Barone, B. Mennucci, M. Cossi, G. Scalmani, N. Rega, G.A. Petersson, H. Nakatsuji, M. Hada, M. Ehara, K. Toyota, R. Fukuda, J. Hasegawa, M. Ishida, T. Nakajima, Y. Honda, O. Kitao, H. Nakai, M. Klene, X. Li, J.E. Knox, H.P. Hratchian, J.B. Cross, V. Bakken, C. Adamo, J. Jaramillo, R. Gomperts, R.E. Stratmann, O. Yazyev, A.J. Austin, R. Cammi, C. Pomelli, J.W. Ochterski, P.Y. Ayala, K. Morokuma, G.A. Voth, P. Salvador, J.J. Dannenberg, V.G. Zakrzewski, S. Dapprich, A.D. Daniels, M.C. Strain, O. Farkas, D.K. Malick, A.D. Rabuck, K. Raghavachari, J.B. Foresman, J.V. Ortiz, Q. Cui, A.G. Baboul, S. Clifford, J. Cioslowski, B.B. Stefanov, G. Liu, A. Liashenko, P. Piskorz, I. Komaromi, R.L. Martin, D.J. Fox, T. Keith, M.A. Al-Laham, C.Y. Peng, A. Nanayakkara, M. Challacombe, P.M.W. Gill, B. Johnson, W. Chen, M.W. Wong, C. Gonzalez, J.A. Pople, Gaussian03, Revision C.02, Gaussian, Inc., Wallingford, CT, 2004.
[42] MOLVIB, Program developed by K. Kuczera and J. Wiorkiewicz-Kuczera at Harvard University, 1990.
[43] H. Gebavi, D. Ristić, N. Baran, L. Mikac, V. Mohaček-Grošev, M. Gotić, M. Šikić, M. Ivanda, Mater. Res. Express 5 (2018), 015015.
[44] A. Michota, J. Bukowska, J. Raman Spectrosc. 34 (2003) 21.
[45] W.-Q. Ma, Y. Fang, G.-L. Hao, W.-G. Wang Chin, J. Chem. Phys. 23 (2010) 659.
[46] A. Dhawan, IEEE Sensors J. 10 (2010) 608–616.
[47] F. Wang, R.G. Widejko, Z. Yang, K. Van, T. Ngyen, H. Chen, L.P. Fernando, K.A. Christensen, J.N. Anker, Anal. Chem. 84 (2012) 8013.
[48] H.-B. Guo, F. He, B. Gu, L. Liang, J.C. Smith, J. Phys. Chem. A 116 (2012) 11870.
[49] M. Pagliai, S. Caporali, M. Muniz-Miranda, G. Pratesi, V. Schettino, J. Phys. Chem. Lett. 3 (2012) 242.